

A new psychophysical estimation of the receptive field size

Arash Yazdanbakhsh^{a,b,*}, Simone Gori^c

^a Cognitive and Neural Systems Department, Boston University, Boston, MA 02215, United States

^b Neurobiology Department, Harvard Medical School, Boston, MA 02115, United States

^c Università degli studi di Trieste, Dipartimento di Psicologia, Via Sant'Anastasio 12, 34133 Trieste, Italy

ARTICLE INFO

Article history:

Received 29 November 2007

Received in revised form 8 April 2008

Accepted 11 April 2008

Keywords:

Receptive field, Visual illusion, Aperture problem, Visual field eccentricity, Psychophysics, Motion, fMRI

ABSTRACT

When a line extends beyond the width of an aperture, its direction of motion cannot be detected correctly. Only the component of motion perpendicular to the line is detectable (aperture problem). Early visual areas face the same aperture problem because receptive field sizes are relatively small. The susceptibility of early visual areas to the aperture problem opens an opportunity to measure the aperture width of a receptive field psychophysically that can be used to estimate the receptive field size. We found an already established visual illusion (the rotating tilted lines illusion or RTLI) can be used to measure the aperture size and hence estimate the receptive field size. To estimate the receptive field size, we conducted a psychophysical experiment in which the radii and tilted line length of RTLI were systematically changed. Our psychophysical estimation of receptive field size strongly corresponds with the previous measures of receptive field size using electrophysiological and fMRI methods.

Published by Elsevier Ireland Ltd.

The cell receptive field (RF) samples a limited area of the visual field as if the cell is looking through an aperture. Therefore, the direction of motion of a line that extends beyond the receptive field is judged to be perpendicular to the line (Fig. 1a). As Fig. 1b shows, if the line length is shorter than the aperture, the true direction of the line motion can be detected [8].

Although it is already known that psychophysical methods can be used to measure the RF size with good approximation [14], we present a new and comparatively simple psychophysical task that approximates the RF size.

In Fig. 1c a circle is composed of tilted lines along its periphery. When the head is moved towards and away from the image, the circle shows apparent rotation [2]. Different aspects of this illusory effect and the involved parameters are fully discussed in the previous works [2,3].

Interestingly, the properties of the illusion itself can be used to measure the receptive field size. Fig. 1d shows the condition where the aperture size is larger than the tilted line. The zoomed insets adjacent to Fig. 1d highlight the angle of the lines composing the illusion and the direction of motion on the retina (radial, due to the back and forth head movements). When the line is smaller than the width of aperture, the radial motion of the line can be detected veridically and the size of the object is perceived to be constant

despite any radial expansion. On the other hand, when the line is larger than the RF only the motion component orthogonal to line is detected (Fig. 1e). This contributes to the perception of rotation, because these lines are perceived to have a motion component tangent to the circle.

We make a functional assumption: the transition from the rotation condition to the no-rotation condition occurs when the lines length changes from being longer than the RF to being shorter than the RF [4,10]. Theoretically, this can provide a method of measuring the functional aperture diameter of the RF and estimate the RF size.

As mentioned in the previous section, the systematic change from long tilted lines into shorter lines at a certain point results in the fading of the illusion. Fig. 2 shows a sequence of stimuli having progressively longer lines.

At a given eccentricity and a fixed RF size, finding the relation between the illusion power and the component-line length yields an estimate of RF aperture size. However, it is known that the RF size scales with eccentricity, therefore it is worthwhile to examine the relationship between RF size and eccentricity.

Each of the stimuli in Fig. 2 has a fixed radius (R) which projects onto the retina with a fixed eccentricity. At a fixed eccentricity and certain RF size (zoomed by a circle in stimulus 3 of Fig. 2) the fading of the perceived illusion would occur around stimulus 3. Testing subjects to find the relation between the illusion power and the tilted line length can give us an estimate of RF aperture size for each eccentricity.

Roughly, it has been estimated that the RF size in V1 (and with less extent of precision in V2 and V3) scales with eccentricity. That

* Corresponding author at: Cognitive and Neural Systems Department, Boston University, 677 Beacon Street, Boston, MA 02215, United States.

E-mail addresses: Arash.Yazdanbakhsh@hms.harvard.edu (A. Yazdanbakhsh), gori@psico.units.it (S. Gori).

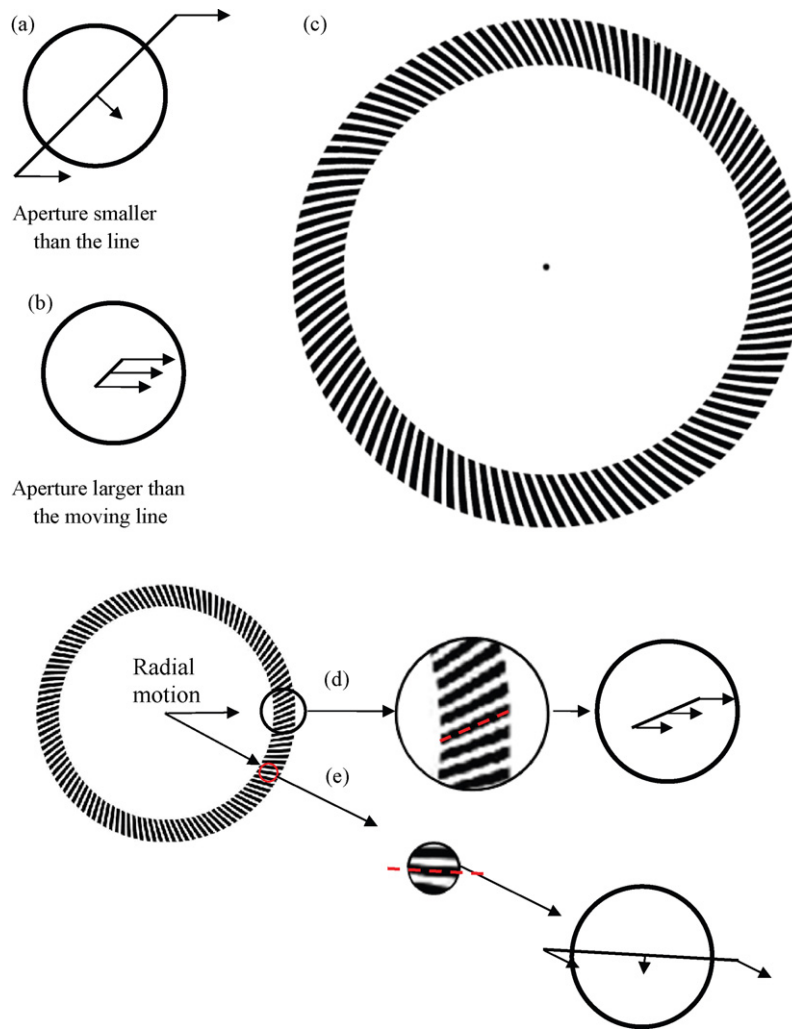


Fig. 1. Receptive field and aperture problem. In (a) the motion being viewed through an aperture is orthogonal to the orientation of the moving line. In (b) the true direction of motion is detectable. (c) The RTLI. By heading toward and away from the stimulus, one perceives clockwise and counter-clockwise rotations. Receptive field size and the RTLI illusion: when the tilted lines are shorter than the aperture size (d), the illusion stops because the lines are within the RF and the true radial direction of motion can be detected. When the cell RF is smaller than the tilted lines (e), only the component of motion orthogonal to the lines orientation is detected and the illusory rotation can be seen.

says, at an eccentricity of Ecc ($^\circ$) if the aperture size of RF is rf ($^\circ$), then the relation between them can be summarized as the following equation [12]:

$$rf = \frac{Ecc + a}{k}$$

where a and k are constants (0.7 and 15, respectively). Although it is a rough estimation, it can be considered a reasonable approximation within the range of eccentricities that we are dealing with here [7,12,13].

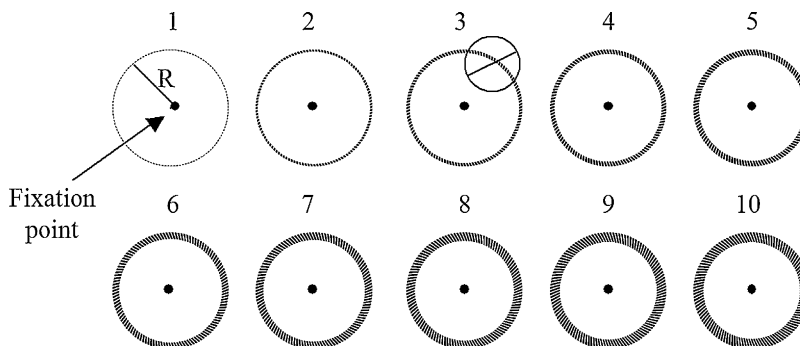


Fig. 2. A subset of stimuli. Looking from stimulus 10 to 1 shows that the illusion strength gets less.

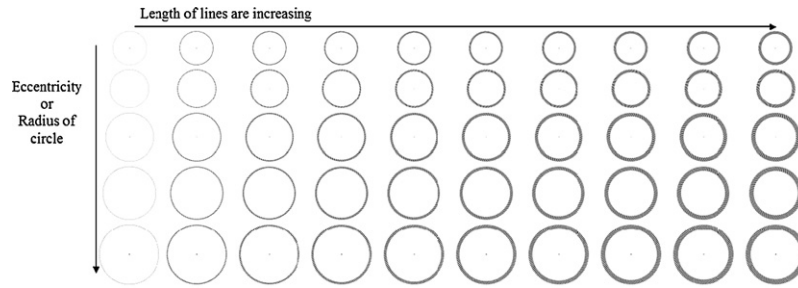


Fig. 3. Full stimuli set. Stimuli at each row have a fix radius. Stimuli at each column have a fix tilted lines length. At each row the tilted line length increases from left to right. At each column the stimulus radius increases from top to bottom.

Fig. 3 shows the full constellation of stimuli with the range of line lengths and eccentricities used to estimate the RF size.

In each trial the subjects were exposed to the stimuli in one row, which contains 10 randomized stimuli. The subject’s task was to report whether the illusory rotation could be seen or not and if it could be seen to rate it from one to five. The subjects were viewing the stimuli binocularly.

In each row, the stimulus consisted of a movie of the expansion and the contraction of the illusion. The expansion and contraction lasted half a second. The radius of each stimulus expanded and

contracted a length equal to half of the maximum bar length of the last stimulus in the row.

The subjects were instructed to rate the rotation of each stimulus in comparison to a reference stimulus which had the strongest effect. The reference stimulus for each row was always the one with the longest tilted lines.

We chose the above method for the following reasons:

- (a) Using the expansion/contraction method allowed us to present stimuli at a fixed distance and control for the variability of each

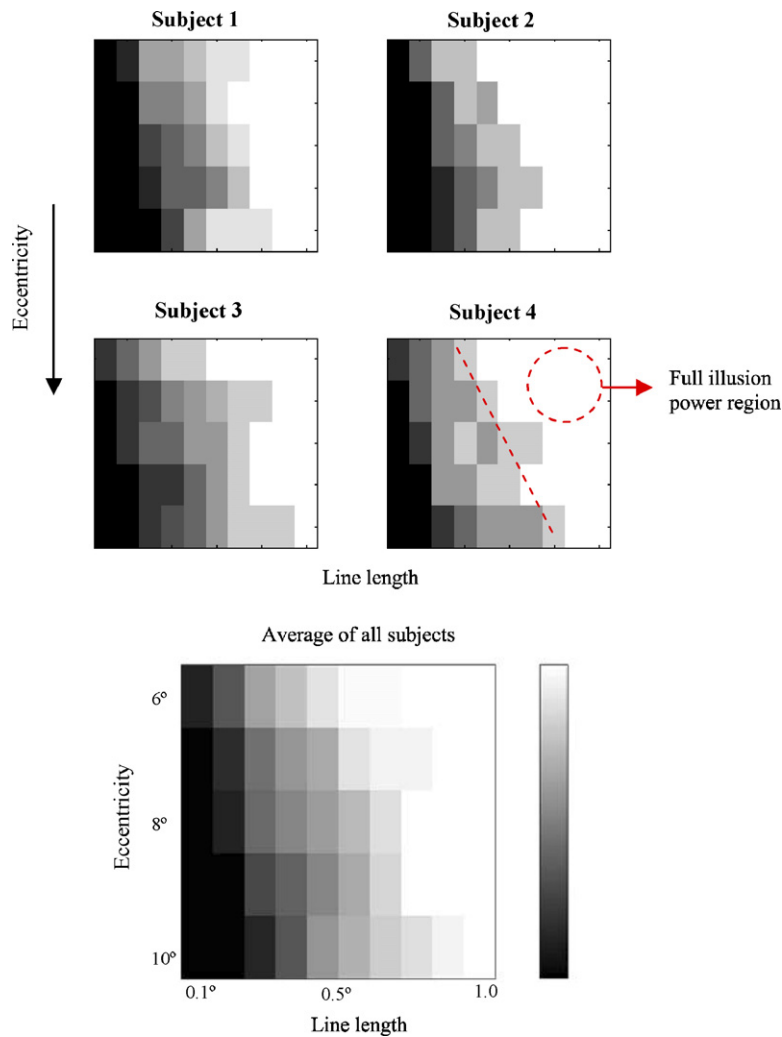


Fig. 4. The results of testing four subjects with the stimuli in Fig. 3. The illusion power is grey-scaled for each line length and eccentricity. White represents 5 and black represents 0.

subject's backward/forward head movement, which plays an important role in the illusion perception and its strength.

- (b) The range of the expansion/contraction is half the length of the line component. This is a minimum amount of expansion/contraction to trigger the illusion vividly. We kept the expansion/contraction at this level to keep any potential confounding factor to a minimum (an example of a confounding factor is that a large radius change causes a significant eccentricity change).
- (c) We chose the longest line at each row as a reference for maximum illusion strength, because it shows the strongest illusion for the desired eccentricity. We did not choose one stimulus as a reference for all rows, but used one reference per each row, to make sure the radius (eccentricity) will not be a confounding factor for strength evaluation of the illusion and each row stimuli are compared with the strongest illusion with the same radius.
- (d) We chose expansion/contraction every half a second, because it was found to be the speed which triggers the illusion most vividly.

Fig. 4 shows the result of such a test for 4 subjects. The score of each stimulus is gray-scaled. Black represents 0 and white represents 5.

As can be seen, the bottom left of each panel of Fig. 4 looks darker, while the top right looks brighter. This basically means that shorter bar lengths are needed for the illusion to fade using stimuli with smaller radii than are needed for stimuli with longer radii.

For clarification, a dotted diagonal line is added to Fig. 4, subject 4.

To get a handle on the line size where the illusion power is $\alpha\%$ of the full illusion power, we used a simple geometrical realization. The average graph of Fig. 4 is plotted in 3D where the illusion power is plotted in Z-axis (Fig. 5a). The x and y axes are the same as in Fig. 4. As can be seen the surface curve is discrete, because the sampling of data points are sparse and not continuous. To obtain a continuous surface curve we used bilinear method of MATLAB to interpolate between the discrete values (Fig. 5b). To find the line-length versus eccentricity relation when the illusion has $\alpha\%$ power, we crossed $z = 5 \times \alpha\%$ plane with the surface curve. We have shown it for four different arbitrary α (Fig. 5b) to see different line-length versus eccentricity curves.

For the range of eccentricity used in our experiments ($6\text{--}10^\circ$), we plotted the RF size versus eccentricity based on $rf = (Ecc + a)/k$ equation ([13]). The points are shown by solid squares in Fig. 5d. By varying α , the $z = 5 \times \alpha\%$ plane intersection with the surface curve in Fig. 5b changes. We chose the intersection curve that passes through the 8° eccentricity solid square (Fig. 5c; this curve is shown by gray-white separation in Fig. 5d). This means we found a

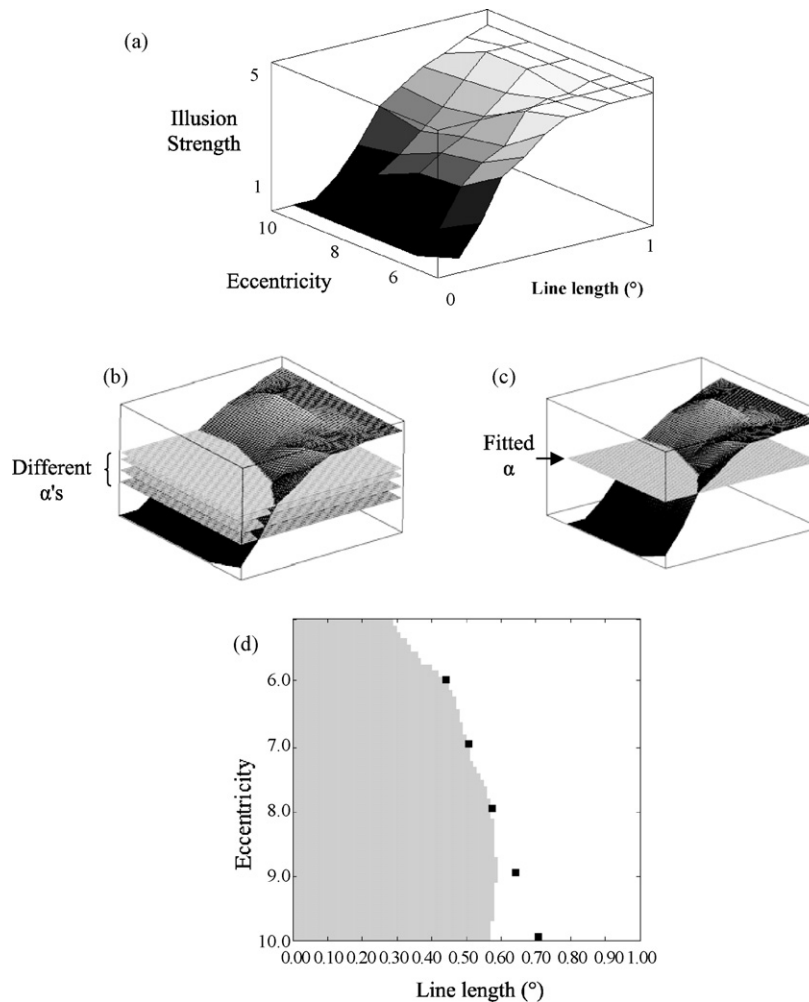


Fig. 5. Fitting the psychophysical data with the RF size data. In (a), the average data in Fig. 4 is represented as a surface curve. The vertical axis (Z-axis) indicates the illusion power. In (b), planes with different Z coordinates are crossed with the surface curve. In (c), one of the planes is selected (see the text). In (d), the intersection curve and the superimposed RF size data (solid squares) are shown.

Table 1
Comparison between RF size and functional estimation by RTLI

Eccentricity (stimulus radius) (°)	Receptive field size (psychophysics) (°)	Receptive field size (electrophysiology) (°)
6.0	0.45	0.45
7.0	0.51	0.51
8.0	0.58	0.58
9.0	0.60	0.65
10.0	0.58	0.71

The comparison between the RF size obtained by using the RTLI and electrophysiological estimation is perfect for smaller eccentricity (6–8°). The potential reason for the smaller functional RF size obtained psychophysically compared to the electrophysiological estimation in anesthetized monkey in larger eccentricities (9–10°) is discussed in the text.

psychophysical curve intersecting the corresponding electrophysiological data at 8° eccentricity.

The question is how the gray-white curve and the solid squares coincide with each other. For eccentricities 6°, 7°, and 8°, these two curves coincide with each other, however, in 9° and 10°, the curves deviate from one another. The RF size, obtained by the equation based on anesthetized monkey data shows a larger value compared with the psychophysical measurement. The potential reasons for such a discrepancy are described in the next section.

The underlying mechanisms of previous versions of RTLI by Pinna and Brelstaff [11] have been scrutinized in a variety of works [3,5,6]. The RTLI is an attractive illusion for psychophysical investigation because it has a single component, tilted lines, with one parameter which is line length. This makes the illusion a good substrate to estimate the size of a RF. We hypothesized that as soon as the length of the lines gets longer than the RF size, the aperture problem takes place, and the direction of motion becomes ambiguous. We used this transition as a basis to measure the RF size.

By varying line length and eccentricity, we obtained a surface curve of the illusion power. By introducing the parameter α or illusion power, we could fit the line length to the electrophysiologically measured RF size. At larger eccentricities the fitted psychophysical RF is smaller than the electrophysiologically measured RF in the anesthetized monkey (Fig. 5d).

One potential reason for this discrepancy can be inferred from Pack et al. [9]. The results from Pack et al. show that neurons in anesthetized and awake monkeys handle the aperture problem in quite different ways. Another potential reason could be that RF is structured differently in humans and monkeys. Therefore the studies that measured RF size using a population receptive field (pRF) estimation in awake human subjects like Dumoulin et al. [1] can shed light on the discrepancy arising between data from the anesthetized monkey [7] and our psychophysical pRF estimation. Dumoulin et al. [1] used functional MRI methods for estimating the neuronal pRF. Their results show non-monotonic changes in receptive field size with increasing eccentricity. Similarly, our results using a psychophysical measure of human pRF shows a non-monotonic trend with increasing eccentricity. This is in stark contrast to the data from Monkeys, which shows an increasing trend of RF size (Table 1). In particular, careful inspection of the data in Fig. 6 of Dumoulin et al. shows that similar to our data, subject C has the same peak at 9° eccentricity with a decreasing trend once the eccentricity increases to 10°.

The minimal line length needed to induce the full strength RTLI is actually larger than would be expected given the electrophysiologically measured RF size. Hence the illusion power parameter α is less than 1. This indicates the information available to a neuron for judging movement actually extends somewhat beyond the aperture expected from the size of the electrophysiological RF. As Fig. 6 shows, when the RF is exposed from the longest bar to the shortest, three stages discussed below take place that show the

decrease in illusion power actually measures the length of the inter-inhibitory zone as an estimate of the activation zone in between.

Stage 1: in the long bar condition, the inhibitory and the activation zones of the receptive field are exposed to the full bar length. This is the stage where the maximal illusion is observed.

Stage 2: while the bar length is decreasing, it approaches to the inter-inhibitory zone length which includes the activation zone and part of both end-inhibitory zones of the RF. In this case, the cells end-inhibitory zones will get the maximal input. This is the potential point at which the power of the illusion begins to perceptually decline. Therefore the embedded activation zone isn't the only source of information for making judgments about motion and the inter-inhibitory region provides a motion estimate.

Stage 3: when the bar length is shorter than the inter-inhibitory zone, the bar is short enough to avoid the aperture problem and the direction of movement can be detected veridically and the illusion is blocked.

Also, as shown in Fig. 5, the aperture sizes estimated from RTLI tend to be smaller than real RF sizes at small eccentricity area (e.g. at 5°, ~0.4° vs. 0.3°). A possible explanation is that neurons at smaller eccentricities tend to have RFs that overlap more with neighboring RFs, leading to a smaller estimated pRF from RTLI.

Another important question is why subjects cannot solve the aperture problem over time. Integrating information from end-stopped neurons to solve the aperture problem may take time, but ultimately it occurs [9]. Thus, if the RTLI stimulus is rapidly expanded and contracted, the rotational illusory percept will be vivid due to the unsolved aperture problem. However, if this expansion and contraction occurs slowly, no rotational percept will occur. To assess the time course of the effect, it is useful to vary (decrease) the speed of the expansion/compression to see if the

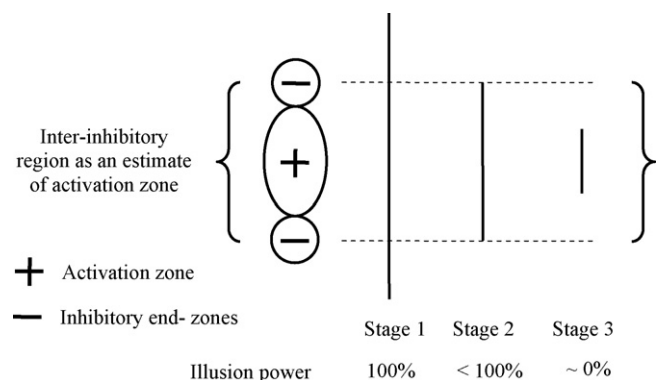


Fig. 6. From the longest bar to the shortest, three stages occur: stage 1, the bar is long enough to span both inhibitory and activation region of the RF. Here the illusion is strong and RF has the aperture problem. In stage 2, the bar size is around the inter-inhibitory length of the RF and therefore the aperture problem is solved by cell's RF. In this stage illusion power declines, and by adjusting α less than 1 we estimate electrophysiological RF size based on the inter-inhibitory zone length. In stage 3, the bar is even shorter, and there is no aperture problem, hence the illusion power remains declined.

hypothesis of giving time to solve the aperture problem works or not. To get the most vivid result, we slowed down the expansion/contraction for the strongest illusion version with long bars ([supplementary movie](#)) by four times, which interestingly resulted in a near to total disappearance of the illusion reported by four subjects. This shows that by giving enough time, the aperture problem is solved.

Using a simple and easily replicable psychophysical task we were able to develop a method that can demonstrate a correspondence between the psychophysical RF and the electrophysiologically and fMRI measured RF.

Acknowledgments

A.Y. was supported in part by NSF grant for CELEST in Cognitive and Neural Systems Department, Boston University and by NIH grant EY13135 to Neurobiology Department (Livingstone Lab), Harvard Medical School.

We thank Anton L. Beer for the valuable communication. We thank Mark Dranias and Michael-John Tavantzis for insightful feedbacks as well as anonymous reviewers for their careful and detailed reading and constructive comments.

Appendix A. Supplementary data

Supplementary data associated with this article can be found, in the online version, at [doi:10.1016/j.neulet.2008.04.040](https://doi.org/10.1016/j.neulet.2008.04.040).

References

- [1] S.O. Dumoulin, B.A. Wandell, Population receptive field estimates in human visual cortex, *Neuroimage* 39 (2) (2008) 647–660.
- [2] S. Gori, K. Hamburger, A new motion illusion: the rotating-tilted-lines illusion, *Perception* 35 (6) (2006) 853–857.
- [3] S. Gori, A. Yazdanbakhsh, The riddle of the rotating tilted lines illusion, *Perception* 37 (4) (2008) 631–635.
- [4] S. Grossberg, E. Mingolla, Neural dynamics of motion perception: direction fields, apertures, and resonant grouping, *Percept. Psychophys.* 53 (3) (1993) 243–278.
- [5] R. Gurnsey, G. Page, Effects of local and global factors in the Pinna illusion, *Vision Res.* 46 (11) (2006) 1823–1837.
- [6] R. Gurnsey, S.L. Sally, C. Potechin, S. Mancini, Optimising the Pinna–Brelstaff illusion, *Perception* 31 (10) (2002) 1275–1280.
- [7] D.H. Hubel, T.N. Wiesel, Uniformity of monkey striate cortex: a parallel relationship between field size, scatter, and magnification factor, *J. Comp. Neurol.* 158 (3) (1974) 295–305.
- [8] J. Lorenceau, M. Shiffrar, N. Wells, E. Castet, Different motion sensitive units are involved in recovering the direction of moving lines, *Vision Res.* 33 (9) (1993) 1207–1217.
- [9] C.C. Pack, R.T. Born, Temporal dynamics of a neural solution to the aperture problem in visual area MT of macaque brain, *Nature* 409 (6823) (2001) 1040–1042.
- [10] C.C. Pack, M.S. Livingstone, K.R. Duffy, R.T. Born, End-stopping and the aperture problem: two-dimensional motion signals in macaque V1, *Neuron* 39 (4) (2003) 671–680.
- [11] B. Pinna, G.J. Brelstaff, A new visual illusion of relative motion, *Vision Res.* 40 (16) (2000) 2091–2096.
- [12] J.R. Polimeni, M. Balasubramanian, E.L. Schwartz, Multi-area visuotopic map complexes in macaque striate and extra-striate cortex, *Vision Res.* 46 (20) (2006) 3336–3359.
- [13] E.L. Schwartz, Spatial mapping in the primate sensory projection: analytic structure and relevance to perception, *Biol. Cybern.* 25 (4) (1977) 181–194.
- [14] L. Spillmann, From perceptive fields to Gestalt, *Prog. Brain Res.* 155 (2006) 67–92.